J. theor. Biol. (1989) **136**, 379–402

Computer Simulation of the Hydrostatic Skeleton. The Physical Equivalent, Mathematics and Application to Worm-like Forms

MARTIN WADEPUHL†

Universität Konstanz, Fakultät für Biologie, Postfach 5560, *D-7750 Konstanz, F.R.G.*

AND

WOLF-JÜRGEN BEYN

Universität Konstanz, Fakultät für Mathematik, Postfach 5560, *D-7750 Konstanz, F.R.G.*

(*Received* 16 *September* 1988)

The functional principles of a hydrostatic skeleton were combined to obtain a physical model which includes geometry, number and length-tension relationships of the elastic elements in the body wall, internal volume and internal pressure. The model skeleton with pre-set internal volume assumes a certain shape and develops a specific internal pressure in order to minimize the potential energy stored in the elastic elements. This shape is calculated as equilibrium state by using finite element methods and optimization techniques. This model is flexible enough to accommodate different geometries and length-tension-relationships of the elastic elements. Presently, the model is implemented with linear length-tension relationships and certain geometrical restrictions, such as uniform width over the entire animal, and rectangular cross sections; the general case is outlined. First simulations with the "unit-worm" yield stable solutions, i.e. stable shapes for all combinations of parameters tested so far. They define the conditions for bringing all muscles to an optimal operating point. We detected a pressure maximum with increasing volume, assessed the contribution of circular muscles to bending, and determined the shapes of animals with different muscle activations in each body half (Chapman-matrix). We summarize our results by the volume rule and stabilization rule, two simple concepts which predict changes in shape as the result of muscle activation.

1. Introduction

Pneumatic constructions are pressurized systems with flexible and stress resistant walls (Otto, 1982). In biology they are better known as hydrostatic skeletons and occur in almost all groups of organisms. Additional knowledge about stability, energy content, and the influence of particular elastic components within the body wall on the shape of the complete structure would facilitate understanding of such diverse biological structures as plant cells (Dierks *et al.*, 1986; Wainwright, 1970), tentacles of hydra (Batham & Pantin, 1950), or the trunk of an elephant (Keir & Smith, 1985). Such a model could also contribute to ideas in evolutionary biology (Gutmann, 1988).

†Present address: Biologie IV, Universität Ulm, Postfach 4066, D-7900 Ulm, F.R.G.

0022-5193/89/040379+24 $03.00/0

This type of construction may not always be obvious. It is present, for example, in arthropods where—although adults are confined within a rigid cuticle—pneumatic principles are transiently important during moulting or are used in later stages to bend certain joints (Alexander, 1979; Barrington, 1979). Also, bones of vertebrates are assumed to gain additional stiffness by incorporation of pneumatic principles (Draenert, 1986).

Hydrostatic skeletons with one or several muscle layers in the body wall are developed in Plathelminthes, Nemertinea, Nematoda, Mollusca and Annelida (see Barrington, 1979, for review).

The functional principles of the hydrostatic skeleton are well understood (e.g. Chapman, 1950). Basically we may think of it as an incompressible fluid enclosed by an elastic body wall. By contraction and relaxation of muscles lying in or inserting at the body wall, the internal pressure and thereby the shape of the whole organism can be changed. Fully contracted muscles are thus elongated by muscles acting as antagonists via the internal pressure. In this way, an amazing variety of body shapes can be generated, which are used in digging, swimming, crawling, ventilation, attachment, etc.

Still, it is difficult to understand the precise physical functioning of a hydrostatic skeleton on a purely intuitive basis, since the activation of one muscle affects, in principle, the length of all others in a way which depends on internal pressure, geometry and length-tension relationship (compare considerations of Chapman, 1950). Direct experimental testing of these intuitions is impossible, since monitoring or manipulating the tension of groups of muscles requires the opening of the body cavity.

It is the purpose of this paper to present a mathematical model for a hydrostatic skeleton which can be handled on a computer. We chose annelids, since their metameric organization and clear arrangement of muscle layers favour such an approach. Our first aim is to adapt this model to simulate the medical leech *Hirudo medicinalis* (L.), which will be presented in a forthcoming paper. We chose this species because its body is not divided by septa and much is already known about its behavior, muscular organization and neuronal control (for review see Muller *et al.*, 1981; Sawyer, 1986). It is, to our knowledge, the first whole body model of a higher animal including all major muscles which influence the shape. By carrying out various simulations with this model and relating them to experimental findings, we hope to achieve a better understanding of the system behavior of this skeleton type. This may also complement neurophysiological investigations which describe muscle co-ordination during certain activities (Ort *et al.* 1974; Kristan *et al.*, 1982; Magni & Pellegrino, 1978) and should allow predictions of muscle co-ordination from kinematic studies (Kristan *et al.*, 1974; Stern-Tomlinsen *et al.*, 1986). In addition, with our approach we can study the effect of activation of each muscle separately, calculate energy consumption and predict internal pressure.

In the next section we derive a physical equivalent of the system, which consists of a sequence of similar segments in which longitudinal and cross sections are quadrilateral. The length of elastic elements situated in the edges of the segments adjust in such a way that the potential energy of the entire system is minimized

under the restriction of a previously chosen constant volume. The following two sections outline how this concept is transformed into a computer simulation by established numerical methods such as finite element analysis and minimization under constraints. Finally, some simulations are presented.

Some aspects of this paper were presented in a preliminary form (Wadepuhl & Beyn, 1987, 1988).

2. The Physical Equivalent of a Hydrostatic Skeleton

Our geometrical substitute of a typical annelid hydrostatic skeleton consists of a sequence of similar segments (Fig. 1). Each of these segments has six faces. The cross and longitudinal sections are quadrilateral. This general form includes the simple case of a sequence of cubes [Fig. 1(a)] as well as the more refined shape shown in Fig. 1(b), which has been adapted to the relaxed state of a leech. We have several reasons for using our geometrical simplification:

(i) It reflects the segmental structure of many annelids.

(ii) It is much simpler to compute deformations of quadrilateral than of, for example, cylindrical objects.

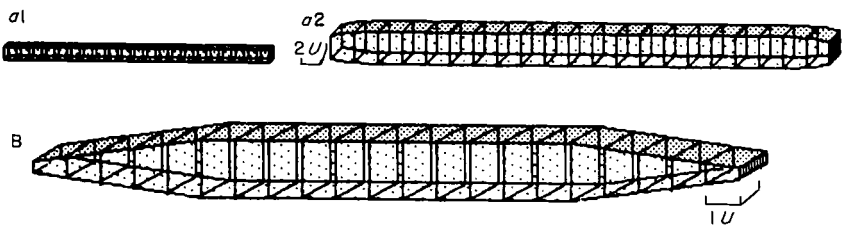

FIG. 1. Minimal length of elastic elements, arrangements of hexahedrals and operating volume. (a1) "unit-worm" inflated with minimal volume, i.e. that volume which is enclosed by elastic elements at its minimal length ($= 1U$). All muscles have the same lengths and length tension curves. Note that no changes in shape are possible in this condition. U = arbitrary length unit. (a2) The same skeleton as (a1) but inflated by 180 arbitrary volume units ($= U^3$). This configuration was used in most simulations. (B) Changes in minimal length allow for adjustment to different body shapes.

(iii) Variation of the length of the edges allows for a high flexibility of the body (see Fig. 11).

(iv) The straight edges of our segments correspond to parts of the muscular system which can be activated separately (cf. Stuart, 1970; Ort *et al.*, 1974). In each segment there are 4 edges representing longitudinal and 8 edges representing circular muscles. In the model, we call these "elastic elements". The 4 lateral edges from the latter group can also incorporate the effects of the dorsoventral muscles. So far, only the oblique muscles have not been directly modelled. Depending on the shape of the body, they may either support the longitudinal or the circular muscles and maintain the pressure (Mann, 1962).

(v) Our model can be thought of as a finite element system using hexahedral elements (Norrie & de Vries, 1978, Section 9), a technique well established in engineering.

Our goal is to compute equilibrium positions of a hydrostatic skeleton. In doing so we neglect all interactions with the environment such as attachment to a surface, hydrodynamic resistence of the medium, and gravity. The last simplification means that we consider only animals living in water, since their specific weight is close to 1 (Jones, 1978). Consequently, we have not taken in account the terminal suckers of the leech.

In a system of N segments with volumes V_i, $i = 1, \ldots, N$, our basic assumption is that the total volume stays constant

$$\sum_{i=1}^{N} V_i = V_{\text{total}}. \tag{2.1}$$

The actual shape of a segment is determined by its 8 corners in the following way: use straight lines to connect first the corners and then corresponding points on opposite edges of the surfaces. Precise formulas will be given in sections 3 and 4. By this geometrical specification we do not allow segmental surfaces to bulge. In this way, we account to a certain extent for the combined stiffness of the epidermis and muscle layers.

Our model has a total of $8N+4$ edges. We assume these to be springs each with a specific length tension relationship, which may depend on the position of the edge within the body. More precisely, following our replacement of the muscles by separate springs, we use the term *force* instead of *tension.* For a typical muscle, we express the force F in terms of the length L and the activation parameter a, which we normalize from 0 to 1.

Figure 2(a) shows a linear relationship between F and L as in Hooke's law, whereas Fig. 2(b) shows a typical non-linear relationship, derived from actual data (Miller, 1975). Passing from the linear to the non-linear case in our simulations can clarify the role of the non-linear length-tension relationship in a hydrostatic skeleton.

In each case, $F(L, 0)$ gives the passive tension curve and $F(L, 1)$ the curve of the isometric maxima. The quantities, which are usually obtained experimentally, are $F(L, 1)-F(L, 0)$ [Fig. 2(b)].

The potential energy stored in a muscle of length L and activation a is obtained by integrating the force

$$P(L, a) = \int_{L_{\min}}^{L} F(l, a)\, \mathrm{d}l. \tag{2.2}$$

Here we have normalized the potential to be zero at the minimal length $L_{\min}$, below which the muscle cannot contract.

The total energy of our hydromechanical system is

$$E_{\text{total}} = \sum_{j=0}^{8N+3} P_j(L_j, a_j), \tag{2.3}$$

where L_j is the length, a_j the activation and P_j the potential function of the jth spring.

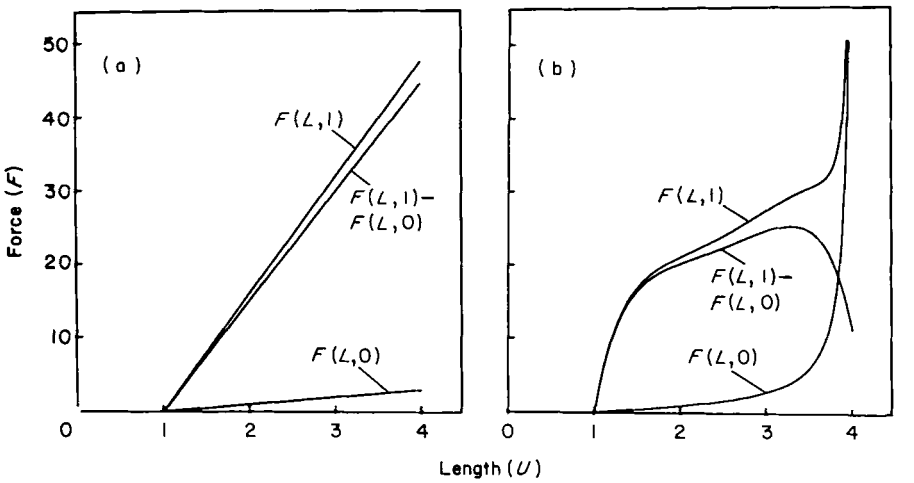

FIG. 2. Force versus length for linear and non-linear elastic elements. (a) Force rises linearly with length of elastic elements used in the "unit-worm" (Hooke's Law). The lines represent length-force relationships of the relaxed $F(L, 0)$ and activated $F(L, 1)$ elastic element. The corresponding constants are 1 and 16, as used for the Chapman-matrix (Figs 13 and 14). The intermediate line shows $F(L, 1) - F(L, 0)$ and correlates with the active length-tension curve in (b). Force equals zero at minimal length ($= 1\,U$). (b) Length-tension curves of leech longitudinal muscles for comparison. Curves fitted to data of Miller (1975) obtained from *Haemopis sanguisuga* L. $F(L, 0)$ denotes passive and $F(L, 1) - F(L, 0)$ active length-tension curve. $F(L, 1)$, curve of isometric maxima. Such curves can also be incorporated into the model.

The equilibrium positions of our system are defined by the minima of the total potential energy under the constraint of constant volume. So only energy differences are relevant during activation and we can assume $E_{\text{total}} = 0$ in the relaxed state, which corresponds to $a_j = 0$ for all j.

Our formulation of an equilibrium position implies a constant hydrostatic pressure p throughout the body (see Section 3). Similar to kinetic gas theory, we have

$$\mathrm{d}E_{\text{total}} = p\,\mathrm{d}V_{\text{total}}. \tag{2.4}$$

This can be interpreted as follows: if we increase against the internal pressure the total volume by $\mathrm{d}V_{\text{total}}$, then we have to supply the energy $p\,\mathrm{d}V_{\text{total}}$. The energy is stored in the elastic elements of the body wall. Hence, the pressure measures the sensitivity of the total energy due to changes in the volume.

The essential features of our model are summarized in Fig. 3.

3. The Mathematical Model in the General Case

In order to make the model from the previous section computable, we must express the total volume and the total energy in terms of one and the same set of variables. In the general case, as shown in Fig. 4 for $N = 4$ segments, we use the

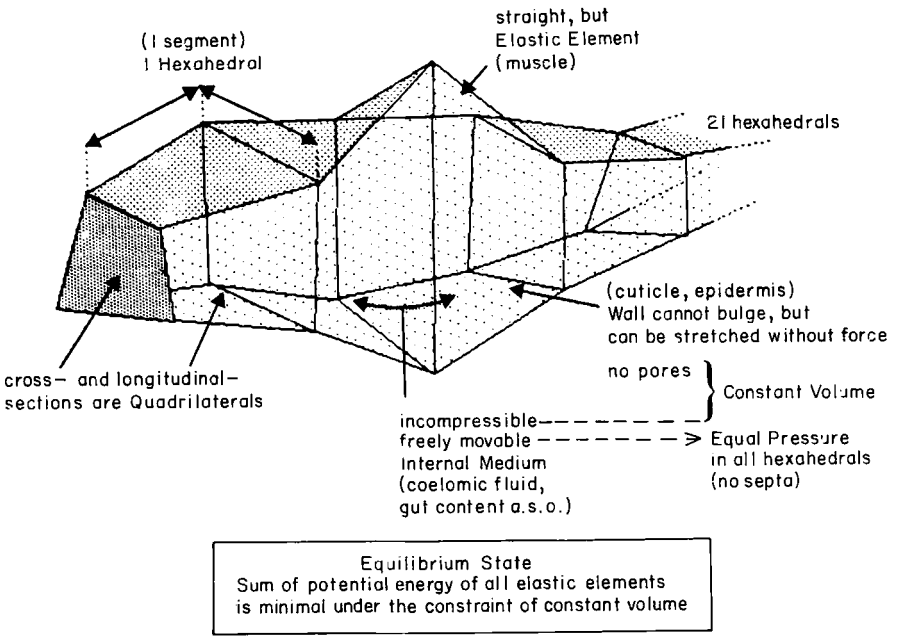

FIG. 3. Summary of essential features of the model. Biological correlates are printed in parentheses. For details see text.

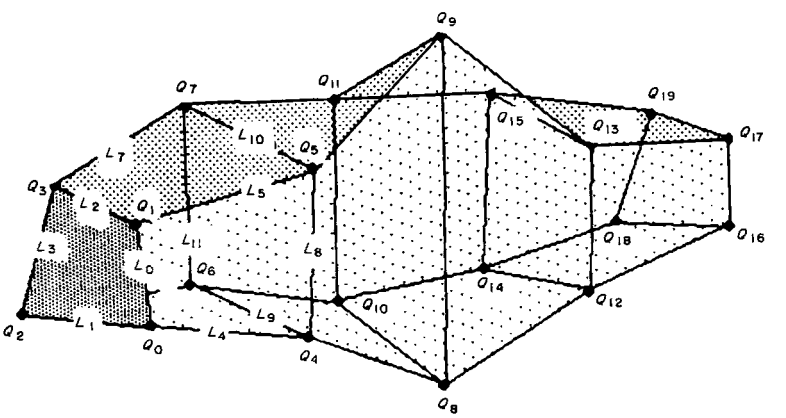

FIG. 4. Skeleton composed of 4 segments, sketched to indicate variables and to demonstrate possible deformation of segments in the general model. For details see text.

co-ordinates of the corners as variables

$$Q_j = (q_{j1}, q_{j2}, q_{j3}), \qquad j = 0, \ldots, 4N+3.$$

Let us look at the first segment S with corners $Q_0, \ldots, Q_7$. As usual in finite element methods (cf., Norrie & de Vries, 1978, Section 9), we describe the segment as the

image of the unit cube under some transformation T (Fig. 5). We take T to be tri-linear.

$$T(x, y, z) = Q_0(1-x)(1-y)(1-z) + Q_1(1-x)(1-y)z + Q_2(1-x)y(1-z) + Q_3(1-x)yz + Q_4x(1-y)(1-z) + Q_5x(1-y)z + Q_6xy(1-z) + Q_7xyz; \qquad 0 \le x, y, z \le 1. \tag{3.1}$$

This mapping meets the physical requirements of the last section because of the following two properties: it maps the corners of the unit cube onto the given corners of the segment, and it maps lines parallel to the co-ordinate axes onto straight lines. It is in fact the only mapping with these two properties. Moreover, any surface is uniquely determined by its 4 corners, so neighboring segments can be put together without penetrating each other.

By the change of variables formula (e.g., Lang, 1968, section 14) the volume of S is

$$V_s(Q_0, \ldots, Q_7) = \int_0^1 \int_0^1 \int_0^1 |J_T(x, y, z)| \, dx \, dy \, dz, \tag{3.2}$$

with the Jacobian determinant

$$J_T(x, y, z) = \det\left(\frac{\delta T}{\delta x}, \frac{\delta T}{\delta y}, \frac{\delta T}{\delta z}\right). \tag{3.3}$$

Using eqn (3.2) we find for the total volume of our model

$$V(Q_0, \ldots, Q_{4N+3}) = \sum_{i=1}^{N} V_s(Q_{4i-4}, \ldots, Q_{4i+3}) \tag{3.4}$$

This functional is rather expensive to evaluate in contrast to the energy functional given by eqn (2.3),

$$E(Q_0, \ldots, Q_{4N+3}) = \sum_{j=0}^{8N+3} P_j(L_j, a_j) \tag{3.5}$$

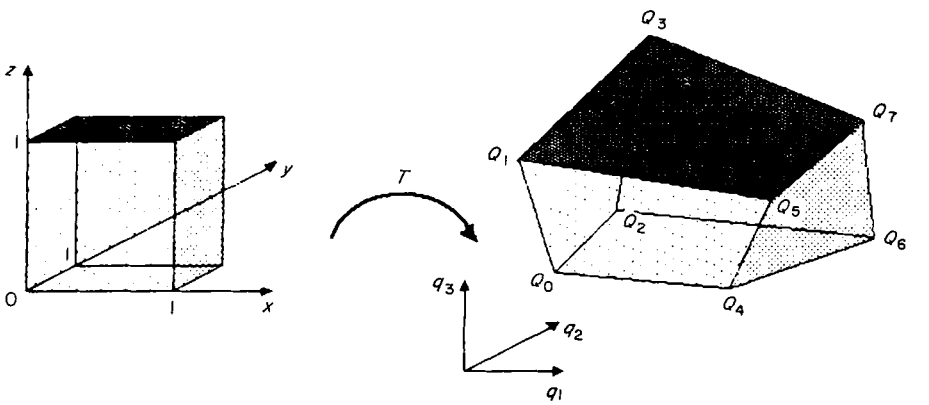

FIG. 5. Transformation of unit cube. For details see text.

Let | | denote the Euclidean length of a vector; then we obtain from Fig. 5 the lengths of the circular muscles as

$$L_j = |Q_{k+1} - Q_k|, \qquad L_{j+1} = |Q_{k+2} - Q_k|, \qquad L_{j+2} = |Q_{k+3} - Q_{k+1}|$$
$$L_{j+3} = |Q_{k+3} - Q_{k+2}|,$$
$$i = 1, \ldots, N+1, \qquad j = 8(i-1), \qquad k = 4(i-1), \tag{3.6a}$$

and the length of the longitudinal muscles as

$$L_{j+4} = |Q_{k+4} - Q_k|, \qquad L_{j+5} = |Q_{k+5} - Q_{k+1}|, \qquad L_{j+6} = |Q_{k+6} - Q_{k+2}|$$
$$L_{j+7} = |Q_{k+7} - Q_{k+3}|,$$
$$i = 1, \ldots, N, \qquad j = 8(i-1), \qquad k = 4(i-1). \tag{3.6b}$$

Our mathematical description of the steady state is then the following constrained minimization problem,

$$\text{Minimize } E(Q_0, \ldots, Q_{4N+3})$$
$$\text{subject to } V(Q_0, \ldots, Q_{4n+3}) = V_{\text{total}}. \tag{3.7}$$

Finally we eliminate the six degrees of freedom, caused by translation and rotation of the body, by requiring

$$q_{01} = q_{02} = q_{03} = q_{11} = q_{21} = q_{23} = 0. \tag{3.8}$$

This fixes Q_0 in the origin, Q_2 on the y-axis and Q_1 in the yz-plane. The complete problem [eqns (3.7) and (3.8)] now has a total of $12N+6$ unknowns (258 if $N=21$).

Any local minimum of eqns (3.7) and (3.8) corresponds to a stable steady state of the whole system, and it is easily seen that such a minimum exists under mild assumptions on E. However, whether these minima are unique depends on the shape of the force functions in respect to the length. If this relationship is linear [as in Fig. 2(a)], several solutions with different degree of stability exist, if the volume is above a critical value. The bifurcation behavior of the problem is under investigation.

At a local minimum of eqn (3.7) there exists a Lagrange multiplier p (e.g. Norrie & de Vries, 1978, section 7) such that

$$\frac{\delta E}{\delta q_{jk}}(Q_0, \ldots, Q_{4N+3}) = p \frac{\delta V}{\delta q_{jk}}(Q_0, \ldots, Q_{4N+3}),$$
$$j = 0, \ldots, 4N+3; \qquad k = 1, 2, 3. \tag{3.9}$$

Comparing this with the total differentials in eqn (2.4), we see that p is exactly the internal pressure. Since common numerical methods for constrained minimization problems also provide estimates of the Lagrange multiplier (Fletcher, 1981) we get the internal pressure as a result of our calculation (see section 5).

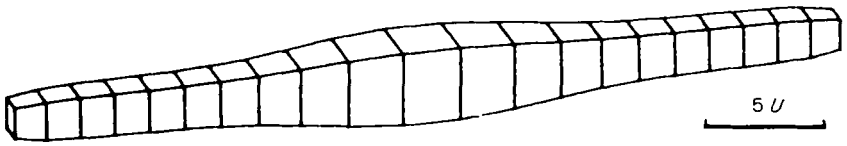

FIG. 6. Shape of unit-worm as calculated by the general model. The volume of $180U^3$ equals 8·57 times minimal volume.

To get a first impression, we show in Fig. 6 the equilibrium state of a 21 segment body, in which all muscles have the same properties.

$$P_j(L, 0) = \tfrac{1}{2}(L-1)^2, \qquad j = 0, \ldots, 171.$$

Although this is certainly an oversimplified situation, we already see that in a relaxed state a body form with an increasing cross section towards the middle seems favorable from an energy standpoint.

The volume was adjusted to

$$V_{\text{total}} = 180$$

of arbitrary units (U^3). Increasing the prescribed volume beyond $243\,U^3$, the multiple solutions appear. Translating the possible multiplicity of stable solutions into biological terms, we must keep in mind that a certain pattern of muscle activation can result in more than one body shape, depending on which was the shape to begin with.

4. The Model with Uniform Width

In this section, we set up a reduced model which essentially restricts the movements of the hydrostatic skeleton to one plane. More precisely, we assume that the body now has a uniform width in all segments and that the cross section of each segment is rectangular (Fig. 7). The geometrical shape of the worm is then specified by the value of the width and by the longitudinal section which consists of a sequence of quadrilaterals.

This reduced model can still represent all co-ordinations requiring movements in the vertical and horizontal plane, since we can take Fig. 7 either as the lateral or the dorsal view of the body. Torsional movements have been excluded by this restriction, but these probably depend on the oblique muscles, which we have neglected anyway.

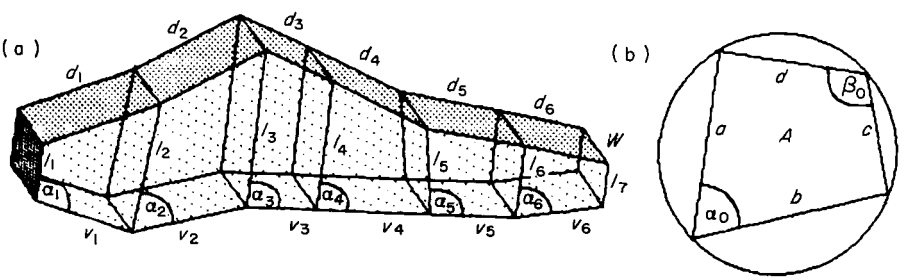

FIG 7. (a) Scheme of a skeleton showing the variables used in the model of uniform width and some possible deformation of segments. For details see text. (b) Notations used in cyclic quadrilaterals.

As for our computations, this simplification considerably reduces the number of variables (from 258 to 65 for a 21-segment worm), so that by a suitable implementation, the system becomes manageable on a Personal Computer. This increases flexibility and reduces cost of computations, which is advantageous when testing multiple combinations of parameters (see section 5). We note, however, differences to equilibrium states calculated with the full model from section 3, which produces different width over the length of the skeleton, in which all muscles have equal properties. It may also be considered as an advantage of the simplified model that, up to now, no instabilities of multiple solutions were detected.

Instead of co-ordinates of corners, we now use as variables the following lengths [see Fig. 7(a)]

$$\begin{aligned} &l_i, \quad i=1,\ldots,N+1 \quad \text{(lateral)} \\ &d_i, \quad i=1,\ldots,N \quad \text{(dorsal)} \\ &v_i, \quad i=1,\ldots,N \quad \text{(ventral)} \\ &w \quad \text{(width).} \end{aligned}$$

We collect these in the $3N+2$ vector

$$x=(l_1, v_1, d_1, \ldots, l_N, v_N, d_N, l_{N+1}, w). \tag{4.1}$$

The total energy eqn (2.3) now has the form

$$E(x)=2\Big\{(N+1)P_c(w, a_w)+\sum_{i=1}^{N+1} P_{ic}(l_i, a_{ic}) + \sum_{i=1}^{N}[P_{iv}(v_i, a_{iv})+P_{id}(d_i, a_{id})]\Big\} \tag{4.2}$$

where the potentials and activations relate to the muscles of each segment as follows,

P_c, a_w: each circular muscle in dorsal and ventral position,
P_{ic}, a_{ic}: ith circular muscle in the two lateral positions,
P_{iv}, a_{iv}: ith longitudinal muscle in the two ventral positions,
P_{id}, a_{id}: ith longitudinal muscle in the two dorsal positions.

We cannot express the volume of our model in terms of the length variables alone, since each quadrilateral needs an additional angle to be completely specified.

Let $A\ (a, b, c, d, \alpha_0)$ denote the formula for the area of the quadrilateral shown in Fig. 7(b). If we introduce the vector of angles $\alpha=(\alpha_1, \ldots, \alpha_N)$ from Fig. 7(a), we find the total volume

$$V(x, \alpha)=w\sum_{i=1}^{N} A(l_i, v_i, l_{i+1}, d_i, \alpha_i). \tag{4.3}$$

The equilibria of the system are then defined by

$$\text{Minimize } E(x) \text{ subject to } V(x, \alpha)=V_{\text{total}}. \tag{4.4}$$

The fact that the α's do not appear in the energy functional suggests that we can eliminate them from the problem. In fact under some natural conditions, the

minimum in eqn (4.4) will always be attained at vectors (x, α), such that $V(x, \alpha)$ has its maximal value for fixed x but variable angles. Suppose that we have a certain length vector x. Then we can vary the vector α to obtain maximal volume. This happens at the minima of eqn (4.4) (see Appendix). The maximal volume occurs exactly if all quadrilaterals have maximum area. The area of a quadrilateral with given sides is maximal if it is cyclic, i.e. inscribed into a circle (see Appendix). The corresponding angle is then given by

$$\cos(\alpha_0) = (a^2 + d^2 - c^2 - b^2)/[2(ad + bc)], \qquad 0 < \alpha_0 < \pi.$$

The area of the cyclic quadrilateral is (Beyer, 1975, section 4)

$$A_c(a, b, c, d) = \tfrac{1}{4}[(a+b+c-d)(a+b-c+d)(a-b+c+d)(-a+b+c+d)]^{1/2}. \tag{4.5}$$

Thus, our minimization problem turns into

$$\text{Minimize } E(x) \text{ subject to } V(x) = V_{\text{total}}, \tag{4.6}$$

where

$$V(x) = w \sum_{i=1}^{N} A_c(l_i, v_i, l_{i+1}, d_i). \tag{4.7}$$

Of course, the length vector x in eqn (4.6) must satisfy some natural additional restrictions, such as positivity and the condition that in each quadrilateral the sum of any three sides is larger than the fourth one.

Our numerical procedure for solving eqn (4.6) was the Lagrange-Newton method, sometimes called the SOLVER method (Fletcher, 1981, section 12), or Wilson's method. It uses Newton's method to compute (x, p) from the Lagrange equations,

$$\frac{\delta E}{\delta x_j}(x) = p \frac{\delta V}{\delta x_j}(x), \qquad j = 1, \ldots, 3N+2, \qquad V(x) = V_{\text{total}} \tag{4.8}$$

In principle, this method starts with a certain set of variables, calculates the slope and curvature of the energy functional and volume functional at this point, and proceeds along this approximation in direction of the unknown minimum.

We took into account the special sparsity pattern of the linear systems arising in each Newton step. Assuming also Hooke's law for the springs, we found a total of approximately $200N$ multiplications per Newton step. Usually 3 to 6 Newton steps were sufficient for the results of the next section.

We also checked the sufficient second order condition for the local minimum of eqn (4.6) and found it satisfied for all simulations quoted in section 5. So we know that all equilibrium positions shown there are stable with respect to small perturbations. However, as in the case of the general model from section 3, we cannot prove that these equilibrium positions are unique in a global sense.

5. Simulations with "Unit Worm"

This section should demonstrate how this model can be employed to study effects of geometry, internal volume and activation of groups of muscles. The simulations are performed with a simplified geometry, whereby minimal length of all muscles in all 21 segments equals unity. This way, general rules about hydroskeletons of worms can be separated from adaptations to a particular species. "Increasing activation" equals "increasing the spring constant" in the following sections.

5.1. OPERATING POINTS OF ELASTIC ELEMENTS

The first set of simulations investigates the development of certain distances within the model due to variation of volume. This corresponds, for example, to the extensive blood meals leeches are known to take (up to 9 times the initial volume, Lent, 1985). By this procedure the length of a medial circular element increases faster than a longitudinal element in the same segment (Fig. 8; see Appendix).

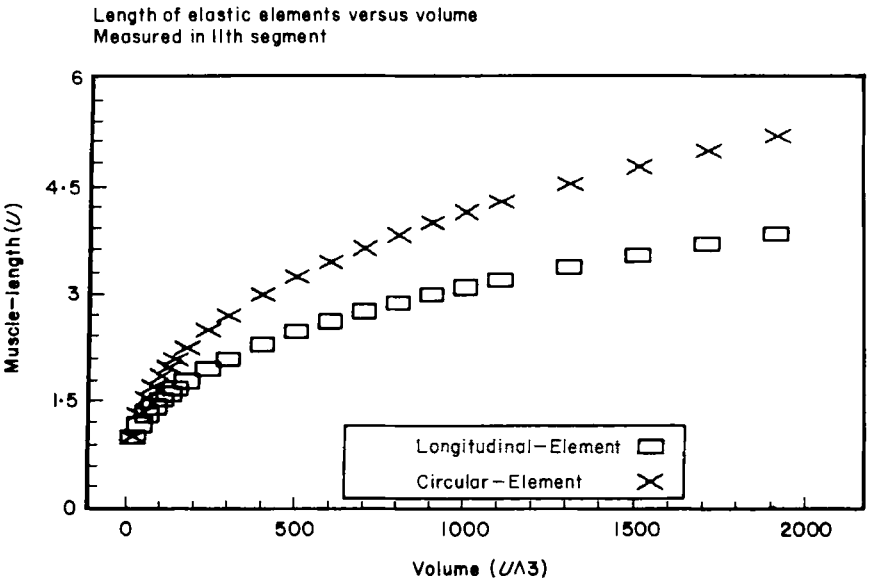

FIG. 8. Length of longitudinal (□) and circular element (×) versus volume. Simulations are performed with unit-worm [Fig. 1(a)], that is, all minimal lengths and all spring constants set to unity. Model of uniform width with 21 segments.

To achieve a maximum of mobility, muscles should be midway between minimal and maximal length. We call this the operating point of the muscle. It would be advantageous if all muscles are at this point in a relaxed animal, since this point can then be reached without expenditure of energy. In our present model, this condition reduces to the claim that with increase of volume, the longitudinal and

circular elements should stretch the same amount, since all muscles have the same properties and no maximum length can be deduced from a linear length-tension relationship.

It is obvious by looking at Fig. 8, however that the "unit-worm" cannot fulfil this criterion. There are three ways out of this dilemma: firstly, the circular elements become stiffer in the relaxed state, which normally means that they become stronger. A second way to bring all muscles in the operating point would be to increase the minimal length of circular elements. Table 1 and Fig. 9 list the changes in the parameters and show that both strategies are successful. The third possibility, the increase of working range toward increased maximal length—which means that circular muscles are more flexible than longitudinal muscles—does not require a change in the unit-worm model. It would certainly be of interest to measure which

TABLE 1

Strategies to reach operating point

Strategies	Unit worm (a)‖		Circular elements: Increase stiffness (b)		Circular elements: Increase length (c)	
Elastic element	LE†	CE‡	LE	CE	LE	CE
Spring-constant $[F/(U-U_0)]$	1	1	1	2	1	0·5
Minimal length (U_0)	1	1	1	1	1	2
Actual length (U) (11th Segment)	1·787	2·250	2·081	2·081	2·086	4·172
Strain $[(U-U_0)/U_0]$	0·787	1·25	1·081	1·081	1·086	1·086
Pressure (F/U^2)	0·6383		1·023		0·2562	

† Longitudinal Element
‡ Circular Element
‖ See Fig. 9.

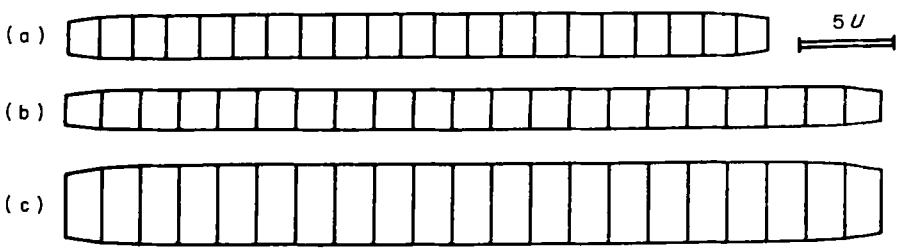

FIG. 9. Two strategies to reach operating point in all muscles. (a) "unit-worm" (see Fig. 8); width and length in medial segment are not equal. (b) "unit-worm" as in (a), but circular elements are stiffer. Now circular and longitudinal elements have equal length. (c) "unit-worm" as in (a), but minimal length of circular elements increased. In order to keep elasticity constant, the spring constant has to be lowered. Volume is increased to 720, which equals 8·57 times minimal volume as in states (a) and (b). As in state (b), both elements have equal strain. See also Table 1. These and the consecutive drawings of the skeleton are side views.

strategies are implemented in hydroskeletons of annelids, with this hypothesis of an optimal operating point in mind.

5.2. ENERGY AND PRESSURE WITH INCREASING VOLUME

Figure 10 plots potential energy of the skeleton versus its volume. For large volumes the energy increases with power of 2/3 of the volume, since length relates to the third root of the volume and the energy grows with the square of the length.

With increasing volume the internal pressure increases sharply at first, levels off, and then decays again, as is expected from the derivative of the energy functional eqn (2.4) (see also Appendix). The shapes are similar to those shown in Figs 1(a) and 9(a).

5.3. BENDING BY ACTIVATION OF LONGITUDINAL ELEMENTS

This section demonstrates the flexibility of a skeleton composed of 21 segments, or 21 finite elements, in technical terms. For the first time, the contribution of the main muscle groups to bending can be assessed. Figure 11 shows the shapes of the skeleton with activation of ventral longitudinal elements increased with factors 2 and 6. Next, all circular elements are activated. For example, an 8-fold increase makes the worm coil twice around its own axis and increases the angle between 2 midbody segments from 18° to 35° (Figs 11 and 12).

Changes in curvature are rapid at first, but decline with increasing activation, independent of the type of elements causing this change (Fig. 12).

These observations can be summarized by the "volume-rule": Whenever elastic elements are activated, they tend to shorten, and therefore transfer, internal volume

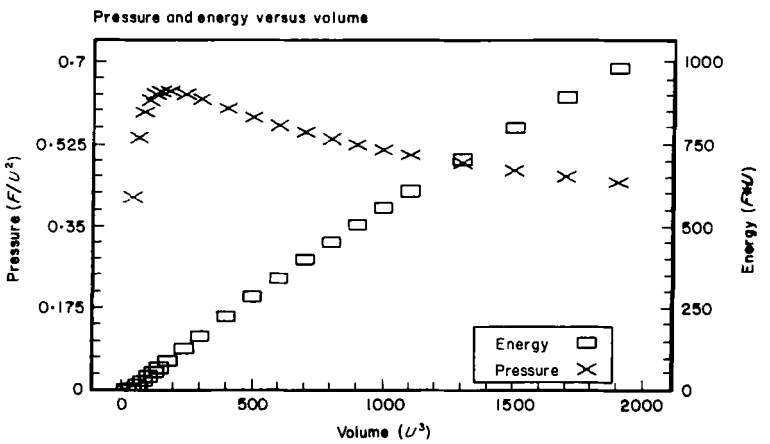

FIG. 10. Pressure (×, left ordinate) and energy (□, right ordinate) of a relaxed "unit-worm" plotted versus stepwise increased volume (same simulations as in Fig. 8).

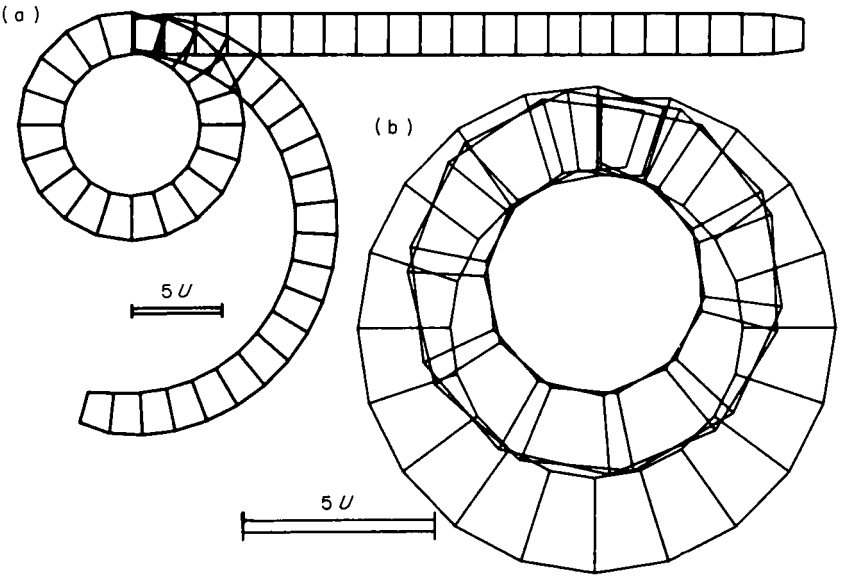

FIG. 11. (a) Body curvature by activation of ventral longitudinal elements with spring constants 1 (straight), 2 (half circle) and 6 (circle). (b) The transition from skeleton forming a single circle [outer skeleton, same as in (a)] to a skeleton coiled twice around itself (inner skeleton) is achieved by activation of all circular elements (spring constant = 8). The segments seem to penetrate each other, due to the lateral view.

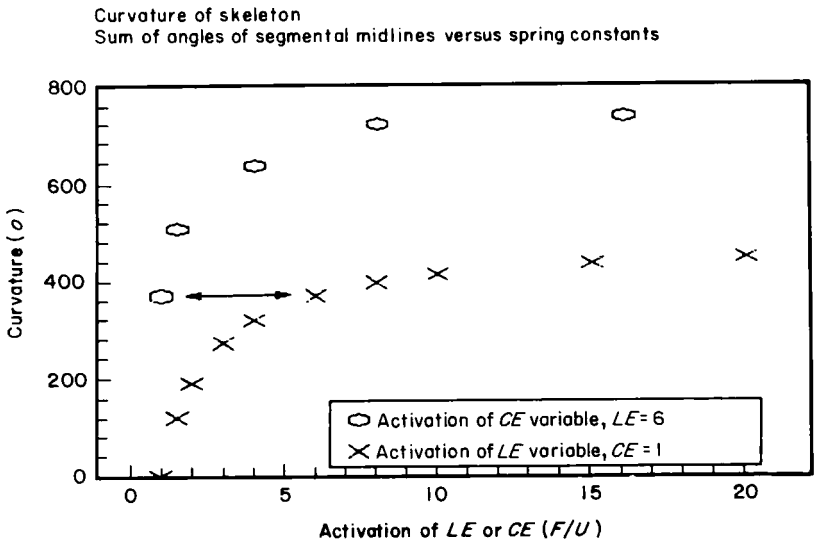

FIG. 12. Curvature plotted against activation of ventral longitudinal elements alone (×) or circular elements (□) in combination with a constant activation of ventral longitudinal elements (spring constant = 6). Symbols connected by double arrow denote values from identical states of the skeleton shown in Figs 11(a), (b).

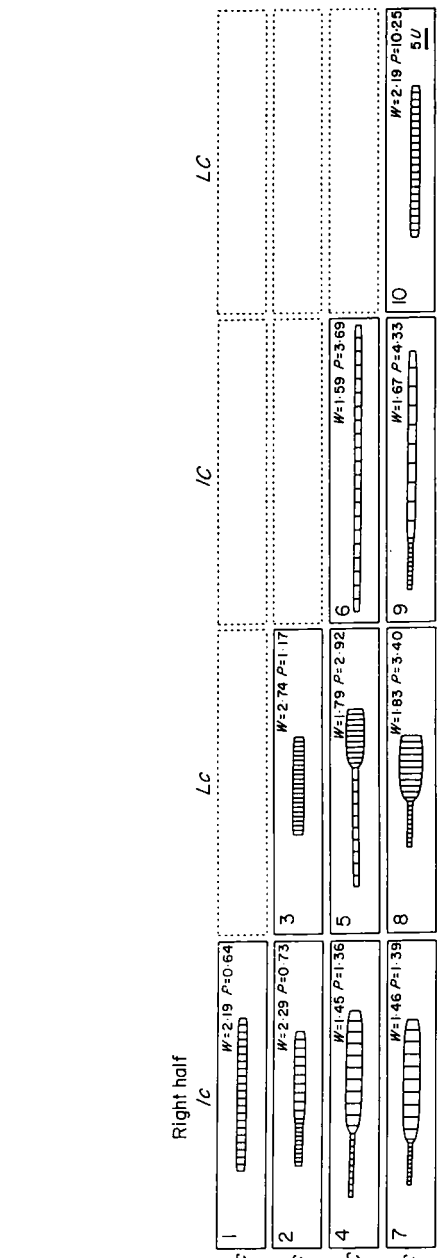

FIG. 13. Chapman Matrix: Simulation of all possible muscle co-ordinations with different activation in each body half. The activation of the right half is constant in each column, while the activation of the left half is constant for each row. The letters symbolize the activation of all longitudinal (l, L) and all circular elements (c, C) in each half. A capital letter stands for a spring constant of 16, a small letter for a spring constant of 1 (= relaxed state). If activation of circular elements differs in each half the spring constant for the width is 8·5. In addition the states are numbered. Stippled frames indicate symmetrical cases. Width (W) and pressure (P) are also given in each frame. The stabilization rule can be observed in the following pairs of co-ordinations: 1–2, 1–4, 2–7, 4–7, 3–8, 5–8, 6–9.

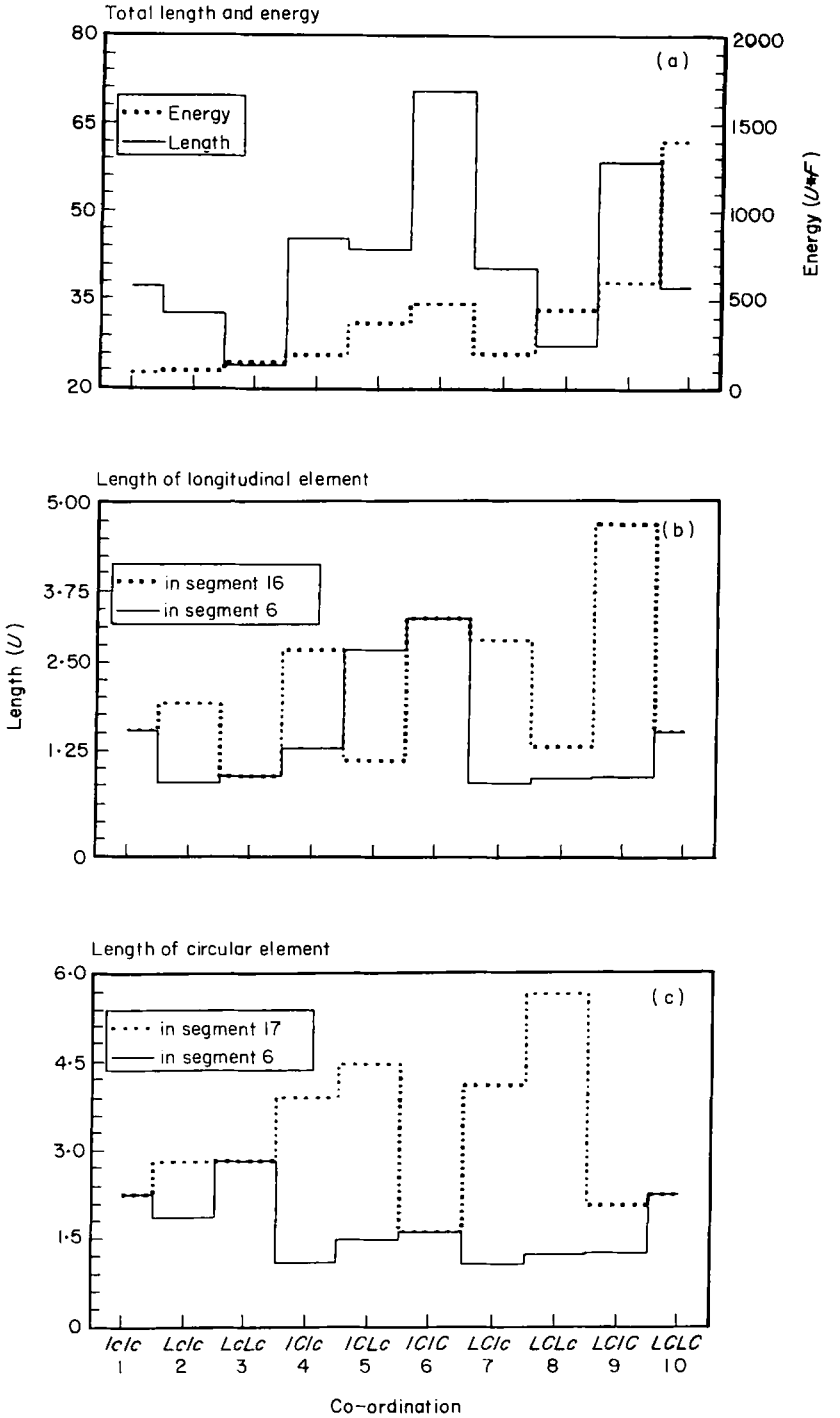

FIG. 14. Energy and lengths in co-ordinations of Chapman matrix. (a) Variation of total length (——) (left ordinate) and energy (· · ·) (right ordinate). Variation of length of dorsal longitudinal (b) and lateral circular (c) element in left [segment 6 (——)] and right half of skeleton [segment 16 or 17 (· · ·), respectively]. The numbers and abbreviations correspond to muscle co-ordinations in Fig. 13.

into regions where the elements are relatively relaxed. In our case, activation of circular elements, combined with activation of ventral longitudinal elements, can only force the volume into spaces provided by elongation of dorsal longitudinal elements which, in turn, coil up the worm even more.

5.4. CHANGES OF ACTIVATION IN HALF OF THE SEGMENTS

Next, we extend the ideas of Chapman (1950), who predicted the shape of a hydroskeleton after activation of groups of muscles within one body half. We simulate systematically all possible configurations (Figs 13 and 14). The spring constants of all activated elastic elements are set to 16.

The results confirm the obvious prediction that activation of either circular or longitudinal elements decreases the diameter or shortens that part of the body, respectively. Activation of all elements to the same degree does not alter the shape.

However, the activation of circular elements in one body half does not lead to elongation, and nor does the activation of longitudinal elements lead to broadening of the activated body half, if compared to the relaxed state. Just the opposite is obtained by simulations.

By comparison of all pairs which differ in the activation of one type of elements in one body half, a regularity emerges, which we call the "stabilization rule": identical muscles with the same activation are shorter, if their neighbors are activated. This rule holds even if the activated neighbors are not orthogonally oriented to the elements under comparison (not shown). This rule can be applied if it is not in conflict with the volume rule; this is certainly the case if the elastic elements under consideration are at least as activated as all remaining elements in the skeleton. Therefore, none of the shapes proposed by Chapman (1950) are obtained, partly because he had to keep one dimension of this model skeleton constant, which is contrary to the principles functioning in a hydroskeleton, and partly because of the effects of the stabilization-rule.

It should also be noted that during intermediate states of bending enforced by circular elements, a shortening of the ventral longitudinal elements is observed according to the stabilization rule.

The unexpected overall shapes demonstrate again that a quantitative model modifies and extends our concepts of the hydroskeleton.

6. Discussion

The model presented provides the first attempt to include geometry, energy, pressure and defined length-tension-relationships in a numerical model of a hydroskeleton. It calculates the shape as an equilibrium state determined by the minimal potential energy of the entire system under the constraint of constant volume within reasonable computing time. The model is highly flexible with respect to the minimal length of the elastic elements, the arrangement and number of the hexahedrals, the length-tension relationship, and the volume. It is now possible to study the effect

of activation of any elastic elements in any combination. Thus the biomechanics of shape-generation and posture of single cells or whole animals can be studied.

6.1. THE RESTRICTIONS WITHIN THE MODEL

Every model must simplify reality in order to obtain new information. Constant volume and equal pressure in all segments are reasonable assumptions for many biological structures (Chapman, 1950). The simulation of animals with pressure compartments, such as segments separated by strong septa in some oligochaetes, would require some modifications of the model.

Equilibrium states of the entire system are valid approximations, especially for slow movements, although in real worms activation of muscles is likely to change before they have reached their equilibrium length. Therefore, a hydroskeleton viewed as a dynamic system needs higher values of activation than the equilibrium model in order to achieve a certain shape.

The main orientation of fibers (muscular or non-muscular) in many hydroskeletons is circular and longitudinal (Chapman, 1958). In some animals helical structures, like the oblique muscles in *Hirudo* (Stuart, 1970) or the inextensible helical fibres in nemertean and turbellarian worms (Clark & Cowey, 1958) are also present. They are, however, mainly responsible for torsional movements (Kier & Smith, 1985) or modulation of pressure (Mann, 1962) and therefore can be neglected in our simulations, while their contribution to bending (Alexander, 1987) is beyond the scope of the present model.

In our system, longitudinal and circular elements are connected, since activation of circular and longitudinal motoneurons produces segmentally restricted contractions in the body wall (Stuart, 1970). The histological substratum anchoring muscle fibres to the surrounding tissue is not yet specified.

Worms without internal muscular systems such as septa or dorsoventral muscles are circular in cross section. Our choice of quadrilateral (general model), or rectangular, cross section reflects mathematical requirements, since arbitrary deformations of a cylinder are very difficult to treat. The choice is, however, justified by the dorsoventral muscles found in the leech, which can account for the deviation from the circular cross section acquired by a pressurized tube. We expect also that segmental sections correspond to cyclic quadrilaterals in most cases, though it is impossible to give exact numbers.

At the moment no interactions with the outside world like gravity, fixation with suckers, or obstacles are incorporated. Our model corresponds to an animal in water, since proteins have a specific weight of 1·2 (Jones, 1978) and worms should therefore have similar weight as water.

We deliberately choose a linear length-tension relationship for our first simulations. In this way, the general behavior of a hydroskeleton can be tested independently of adaptations to a particular animal. The consequences of specializations may then more easily be understood. The detection of bifurcations in the general model, which means different shapes of the skeleton with the same set of muscle activation, can help to understand the shape of the length-tension-curve of leech

muscles. Studies on this problem are in progress. The Chapman-matrix serves as another example of the need to simplify: a different geometry or non-linear length-tension-relationships could interfere with the effects of the stabilization rule.

6.2. THE CONCEPT OF OPERATING POINT

To our knowledge neither the relationship of the length of longitudinal to circular muscles nor the operating points of the muscles have yet been determined for annelids. Deviations from the above presented working hypothesis then suggest different ecological requirements. The strategy, which employs changes in minimal length of circular elements works at the lowest pressure, and therefore seems most advantageous to bring all muscles to the operating point [Table 1, Fig. 9(b)].

6.3. THE PRESSURE MAXIMUM AND LAPLACE' LAW

From Fig. 10 we see that with large volumes ($>200U^3$) the pressure is inversely proportional to length in a first approximation. This is reminiscent of Laplace' law of drops with constant surface tension (see Thompson, 1971). The initial sharp rise in pressure results, on the contrary, from the increase in tension near minimal length.

It should now be obvious that these changes in length or pressure accompanied with increasing volume are difficult to predict without a model, even in the simplified case of a "unit-worm".

6.4. ANOTHER PREDICTION ABOUT NEURAL CO-ORDINATION: BENDING SUPPORTED BY CIRCULAR MUSCLES

Simulations of the control of curvature demonstrated the considerable influence of tension in circular elements. A similar statement was put forward by Keir & Smith (1985), but was based on a different mechanism. Our explanation, the volume rule, should hold for many similar problems.

In addition, semi-quantitative statements are possible. Spring constants exceeding 10 times resting state hardly increase the curvature. However, 50% of the maximum curvature is already achieved by twice the resting spring constant. If this can be validated for other co-ordinations, motoneurons need not produce large forces and should be tuned precisely for economic use of the animals energy resources.

6.5. THE CHAPMAN-MATRIX AND SEARCHING POSTURE

It is obvious that a regularity like the stabilization rule cannot be found by experimentation, since activation of muscles cannot be controlled sufficiently in the intact animal.

The foraging posture of the leech (Sawyer, 1981) is achieved by contraction of the circular muscles in one half, and the longitudinal muscles in the other (co-ordination $lCLc = 5$, Fig. 13). It produces an animal with a wide and short posterior body half, which provides the base for the searching movement of the long and

thin anterior body. An attempt to increase the length of this body by co-contraction of the longitudinal elements should be tuned finely, since it may result in a long, but thick, anterior body as co-ordination 9 (=*LClC*, Figs 13 and, 14).

However, exact predictions are difficult, since we expect that the effects of the stabilization rule are even more drastic if the restriction of uniform width present in the simplified model is no longer valid.

We can further conclude from this matrix that a factor of 16 times minimal tension is certainly not enough for the leech to reach its maximal extension [*Hirudo* reaches up to 6 times minimal body length in swimming (Miller & Aidley, 1973; Lanzavecchia *et al.*, 1985)].

Finally, we want to point out that the model skeleton returns to its original shape upon relaxation of formerly activated muscles, without activation of supposed "antagonists" (Chapman, 1950). How fast this occurs in reality depends of course on the elastic forces in comparison to the viscosity of the tissue.

The stabilization rule together with the effects of pressure on muscle length discussed in Wadepuhl & Beyn (1987) render the notion of "antagonistic" muscles obsolete. Instead, internal pressure is antagonistic to both groups of muscles.

Three different mechanisms are therefore at hand to increase muscle length within a hydroskeleton: (i) the activation of the particular muscle is decreased, (ii) the internal pressure is increased by the action of any other muscle, and (iii) the muscles around the particular muscle decrease their tone.

These first simulations produce not only rules, simplifying the prediction of the outcome of muscle co-ordinations, but elucidate the geometry of worm-like creatures. They also demonstrate that even the simplified "unit-worm" exhibits phenomena not easily assessed by intuitive thinking.

We thank Professor W. Nachtigall for encouragement throughout the project, Dr R. Blickhan for comments on the manuscript and M. A. Cahill for improving the English.

REFERENCES

ALEXANDER, P. (1979). *The invertebrates.* Cambridge: Cambridge University Press.

ALEXANDER, M. R. (1987). Bending of cylindrical animals with helical fibres in their skin or cuticle. *J. theor. Biol.*, **124,** 97-110.

BARRINGTON, E. J. W. (1979). *Invertebrate structure and function.* Wokingham: Van Nostrand Reinhold.

BATHAM, E. J. & PANTIN, C. F. A. (1950). Muscular and hydrostatic action in the sea-anemone *Metridium senile* (L.). *J. exp. Biol.* **27,** 264-288.

BEYER, W. H. (1975). *Handbook of mathematical sciences.* West Palm Beach: CRC Press.

CHAPMAN, G. (1950). On the movement of worms. *J. exp. Biol.* **27,** 29-39.

CHAPMAN, G. (1958). The hydrostatic skeleton in the invertebrates. *Biol. Rev.* **33,** 338-364.

CLARK, R. B. & COWEY, J. B. (1958) Factors controlling the change of shape of certain nemertean and turbellarian worms. *J. exp. Biol.* **35,** 731-748.

DIERKS, K., HAFNER, L., TIETGE, H.-W. & WENDERLING, R. (1986). Zum Trageverhalten des Alpenveilchens. *Symposium on cellular mechanics. Konzepte SFB 230* **18,** 25-29.

DRAENERT, K. (1986). Der Knochen als hydraulisches System. *Pneu und Knochen II. Konzepte SFB 230* **14,** 63-71.

FLETCHER, R. (1981). *Practical methods of optimization.* Chichester, New York: Wiley.

GUTMANN, W. F. (1988). The hydraulic principle. *Am. Zool.* **28,** 257-266.

JONES, H. D. (1978). Fluid skeletons in aquatic amd terrestrial animals. In: *Comparative physiology* (Schmidt-Nielson, K., ed.) pp. 267-281. Cambridge: Cambridge University Press.

KIER, W. M. & SMITH, K. K. (1985). Tongues, tentacles and trunks: the biomechanics of movement in muscular-hydrostats. *Zool. J. Linnean Soc.* **83**, 307-324.
KRISTAN, W. B., JR., MCGIRR, S. J. & SIMPSON, G. V. (1982). Behavioural and mechanosensory neurone responses to skin stimulation in leeches. *J. exp. Biol.* **96**, 143-160.
KRISTAN, W. B., JR., STENT, G. S. & ORT, C. A. (1974). Neuronal control of swimming in the medicinal leech. I. Dynamics of the swimming rhythm. *J. Comp. Physiol. A* **94**, 97-119.
LANG, S. (1968). *A second course in calculus* (2nd ed.) Reading: Addison Wesley.
LANZAVECCHIA, G., DE EGUILEOR, M. & VALVASSORI, R. (1985). Superelongation in helical muscles of leeches. *J. Muscle Res. Cell Mot.* **6**, 569-584.
LENT, C. M. (1985). Serotonergic modulation of the feeding behavior of the medicinal leech. *Brain Res. Bull.* **14**, 643-655.
MANN, K. H. (1962). *Leeches (Hirudinea). Their structure, physiology, ecology and embryology.* New York: Pergamon Press.
MAGNI, F. & PELLEGRINO, M. (1978). Patterns of activation and the effect of activation of the fast conducting system on the behavior of unrestrained leeches. *J. exp. Biol.* **76**, 123-135.
MILLER, J. B. (1975). The length-tension relationship of the dorsal longitudinal muscle of the leech. *J. exp. Biol.* **62**, 43-53.
MILLER, J. B. & AIDLEY, D. J. (1973). Two rates of relaxation in the dorsal longitudinal muscle of a leech. *J. exp. Biol.* **58**, 91-103.
MULLER, K. J., NICHOLLS, J. G. & STENT, G. S. (1981). *Neurobiology of the leech.* Cold Spring Harbor: Cold Springer Harbor Laboratory.
NORRIE, D. H. & DE VRIES, G. (1978). *The finite element method.* New York, London: Academic Press.
OTTO, F. (1982). *Natürliche Konstruktionen.* Stuttgart: Deutsche Verlagsanstalt.
ORT, C. A., KRISTAN, W. B. JR. & STENT, G. S. (1974), Neuronal control of swimming in the medicinal leech. II. identification and connections of motor neurons. *J. Comp. Physiol. A* **94**, 121-154.
SAWYER, R. T. (1981). Leech biology and behavior. In: *Neurobiology of the leech.* (Muller, K. J., Nicholls, J. G., Stent, G. S., eds) pp. 7-34. Cold Springer Harbor: Cold Spring Harbor Laboratory.
SAWYER, R. T. (1986). *Leech biology and behaviour* Vol. I-III. Oxford: Clarendon Press.
STUART, A. E. (1970). Physiological and morphological properties of motoneurones in the central nervous system of the leech. *J. Physiol., Lond.* **209**, 627-646.
STERN-TOMLINSEN, W., NUSBAUM, M. P., PEREZ, L. E. & KRISTAN, W. B., JR. (1986). A kinematic study of crawling behavior in the leech, *Hirudo medicinalis. J. Comp. Physiol. A* **158**, 593-603.
THOMPSON, D'ARCY, W. (1971). *On growth and form.* (Bonner J. T., ed.) pp. 346. Cambridge: Cambridge University Press.
WADEPUHL, M., & BEYN, W.-J. (1987). Computersimulation des Hydroskeletts bei Anneliden. *Verh. Dtsch. Zool. Ges.* (Barth, F. G. & Seyfarth, E., eds) p. 265. Stuttgart; New York: Fisher.
WADEPUHL, M. & BEYN, W.-J. (1988). Neural control of a hydroskeleton: Predictions based on a computermodel. *Verh. Dtsch. Zool. Ges.* (Barth, F. G. & Seyfarth, E., eds) pp. 216-217. Stuttgart; New York: Fisher.
WAINWRIGHT, S. A. (1970). Design in hydraulic organisms. *Naturwissenschaften.* **57**, 321-326.

APPENDIX

Elimination of Angles for the Model of Uniform Width

Let $x_{\min}$ denote the vector of minimal lengths and assume that our system is pressurized, i.e. $V(x_{\min}, \alpha) < V_{\text{total}}$ for all angle vectors α. We consider vectors $\hat{x} > x_{\min}$ ($>$ means greater in each component) and $\hat{\alpha}$ at which eqn (4.4) has its global minimum. Then we claim that

$$V(\hat{x}, \hat{\alpha}) = \operatorname*{Max}_{\alpha} V(\hat{x}, \alpha). \tag{A1}$$

If this is not the case, we find some $\alpha_0 \neq \hat{\alpha}$ satisfying

$$\operatorname*{Max}_{\alpha} V(\hat{x}, \alpha) = V(\hat{x}, \alpha_0) > V(\hat{x}, \hat{\alpha}) = V_{\text{total}}.$$

Now $V(x_{\min}, \alpha_0) < V_{\text{total}} < V(\hat{x}, \alpha_0)$ implies that we find a length vector x_0 such that $x_{\min} < x_0 < \hat{x}$ and $V(x_0, \alpha_0) = V_{\text{total}}$. Using the strict monotonicity of the energy

functional, we obtain $E(x_0) < E(\hat{x})$ which contradicts our assumption that eqn (4.4) has its minimum at $\hat{x}$, $\hat{\alpha}$.

Cyclic Quadrilaterals have Maximum Area

The area of a general quadrilateral with sides a, b, c, d and two opposite angles α_0 and β_0 [Fig. 7(b)] is given by (cf. Beyer, 1975, p. 190),

$$\tfrac{1}{4}\{(a+b+c-d)\,.\,(a+b-c+d)\,.\,(a-b+c+d)\,.\,(-a+b+c+d) - 16abcd\cos^2[\tfrac{1}{2}(\alpha_0+\beta_0)]\}.$$

For fixed values of a, b, c and d this expression clearly becomes maximal if $\alpha_0+\beta_0=\pi$. In this case, the quadrilateral is cyclic and we obtain the formula (4.5).

Operating Point

We consider a simplified system of N equal parallelepipeds each of the length l, width w and height h. Then the condition for an equilibrium is

$$\begin{aligned} \text{Minimize} \quad & 4Na_l(l-l_0)^2+2(N+1)[a_w(w-w_0)^2+a_h(h-h_0)^2] \\ \text{subject to} \quad & Nlwh = V_{\text{total}}. \end{aligned} \tag{A2}$$

Here Hooke's law was assumed for each elastic element. Introducing the extension factors $x=l/l_0$, $y=w/w_0$, $z=h/h_0$ and the constants

$$a_x = 4Na_l l_0^2, \qquad a_y = 2(N+1)a_w w_0^2, \qquad a_z = 2(N+1)a_h h_0^2, \tag{A3}$$

$$v = V_{\text{total}}/(Nl_0b_0h_0),$$

the problem in eqn (A2) becomes

$$\text{Minimize } E(x,y,z) = a_x(x-1)^2+a_y(y-1)^2+a_z(z-1)^2 \text{ subject to } xyz = v. \tag{A4}$$

For each $v \geq 1$ this problem has a unqiue solution x, y, $z \geq 1$ which by Lagrange's eqn [see eqn (4.8)] satisfies

$$2a_x x(x-1) = 2a_y y(y-1) = 2a_z z(z-1) = pv, \tag{A5}$$

where p denotes the pressure.

From eqn (A5) we see that the extension factors x, y, z are in reverse order to the factors a_x, a_y, a_z. If as in the unit worm, we have $a_x = 4N > 2(N+1) = a_y = a_z$ then we find $x < y = z$, i.e. the circular muscles stretch further than the longitudinal muscles.

Equation (A5) also shows that the operating point (defined by $x=y=z$) is obtained if $a_x = a_y = a_z$. By eqn (A3) this requires

$$\frac{2N}{N+1}\, a_l l_0^2 = a_w w_0^2 = a_h h_0^2. \tag{A6}$$

Keeping $a_l = 1$, $l_0 = 1$ as in the unit worm, we see that the operating point can be achieved by increasing either the strength (a_w, a_h) or the minimal length (w_0, h_0) of the circular muscles (compare Table 1).

Pressure diagram

Let us assume the operating point condition eqn (A6) and study the dependence of x, y, z and p on the relative volume v.

From eqns (A4) and (A5) we find

$$x = y = z = v^{1/3}, \qquad p(v) = 2a_x v^{-2/3}(v^{1/3} - 1), \qquad v \geq 1. \tag{A7}$$

The pressure has a maximum at $v = 8$ which corresponds to $x = y = z = 2$. The energy curve is found by integrating p [see eqn (2.4)],

$$E(v) = 3a_x(v^{2/3} - 2v^{1/3} + 1).$$

The plots of these functions (not shown) strongly resemble the energy and pressure curves found for the relaxed unit worm (Fig. 10). One can show that the pressure maximum in eqn (A2) also occurs without the assumption (A6), but we have no explicit formula for this case.

Finally we note that the occurrence of a pressure maximum certainly depends on the length-tension relationship. We take, for example, $E(x, y, z) = \mathrm{f}(x) + \mathrm{f}(y) + \mathrm{f}(z)$ in eqn (A4), where f is a potential function satisfying $\mathrm{f}(1) = 0$, $\mathrm{f}(x) > 0$ for $x > 1$.

Then eqn (A7) generalizes to

$$p(v) = v^{-2/3}\mathrm{f}'(v^{1/3})$$

Using the force function $\mathrm{f}'(x) = \tan(x - 1)$ (which is closer to experimental findings than Hooke's law, see Fig. 2) an easy calculation shows that $p(v)$ is now strictly increasing. Hence, in this case there is no pressure maximum.